Localized metallic melting and hole boring by laser guided discharges

R. M. Gilgenbach, O. E. Ulrich, and L. D. Horton

Department of Nuclear Engineering, The University of Michigan, Ann Arbor, Michigan 48109

(Received 18 August 1982; accepted for publication 6 October 1982)

We demonstrate a new technique for localized melting and boring of materials using discharges guided by laser induced breakdown of atmospheric pressure air. This technique has important applications to a novel method for machining and welding materials, since the melting location can be controlled by adjusting the path of the focused laser beam. These experiments have demonstrated several features of localized metallic melting by laser guided discharges: (1) the melted spot can be scanned by changing only the position of the laser focal spot on the metal sample; (2) the melted spot diameter and profile depend upon the relative timing of the laser pulse and the discharge; (3) defocusing the laser beam has an effect upon the melted spot pattern; and (4) hole boring has been accomplished in aluminum foils which cover the stainless-steel electrode.

PACS numbers: 52.50.Jm, 52.80.Mg, 52.80.Pi, 52.80.Dy

INTRODUCTION

The characteristics of laser guided discharges in air have been studied extensively by a number of researchers.[1-4] Experiments performed at the Naval Research Labs by Greig *et al.*[1] demonstrated that electrical discharges can be initiated and guided by laser induced breakdown at angles almost perpendicular to the applied electric field and even around a 90° bend.[2] Previous investigations elsewhere have shown that this technology has application to laser triggered switches and to particle beam transport systems for inertial confinement fusion reactors.[1,5-7]

We demonstrate here the new application of laser guided discharges (LGD) to machining, and hole boring of materials. There are a number of advantages of this proposed new technique over simple laser machining[8] or electric discharge machining (EDM).[9] Several advantages of laser guided discharges over laser machining are: (1) the pulsed laser energy levels required for LGD are below those necessary for material melting, (2) the electrical efficiency is potentially higher, due to the direct ohmic conversion of electrical energy to thermal energy, rather than the electrical–optical–thermal conversion required in laser machining, and (3) the use of LGD could provide more efficient machining of smooth, metallic surfaces which may reflect a large fraction of incident laser power (this is demonstrated in Sec. III).

There are also numerous advantages of laser guided discharge machining over simple electric discharge machining including: (1) remote, stationary placement of electrodes is possible, since the discharge path is "steerable" by means of the mirror which focuses the laser beam. (2) the discharges can be guided regardless of the direction of the electric field, permitting components to be machined in locations inaccessible to electrodes, such as inside corners, and (3) more accurate machining may be possible, since the discharge can be focused by means of the laser focus.

We have demonstrated the feasibility of this process by producing localized melting and hole boring in metal samples using laser guided discharges. We have shown that several of the aforementioned advantages can be achieved.

I. EXPERIMENTAL CONFIGURATION

The parameters of this experiment were chosen to demonstrate the feasibility of controlled, localized, metallic melting and hole boring by laser guided discharges using existing equipment in our laboratory. Improvements which could be made to increase the efficiency and accuracy of the process are discussed at the end of this article. Figure 1 depicts, schematically, the basic configuration of the experiment. The high-power CO_2 laser (Lumonics Model 601A) generated 100-ns triangular pulses with a total energy of about 12 J.

To demonstrate the effect of laser guided discharge melting on the metal surface, the incident laser power was adjusted to the minimum value (about 6.4 J) required for effective guidance. The incident laser power was controlled by adjusting the propylene pressure in an absorption cell. A 2.5-m focal length mirror with precision vernier adjustments focused the laser beam to the point on the sample which was to be melted. The laser intensity must be slightly above the air-breakdown threshold in order to generate a series of breakdown beads which initiate and guide the discharge across a 3-cm interelectrode gap. At these power levels, the focused laser intensity, after attenuation by the air-breakdown plasma, was below the damage threshold for the stainless-steel and aluminum foil samples employed in these experiments. However, some surface oxidation was observed on samples from air-breakdown plasma at the surface. The CO_2 laser was always pulsed prior to the discharge in these experiments to form a preionized path before the voltage was applied. This ensured discharge guidance and eliminated the prob-

 0034-6748/83/010109-05$01.30

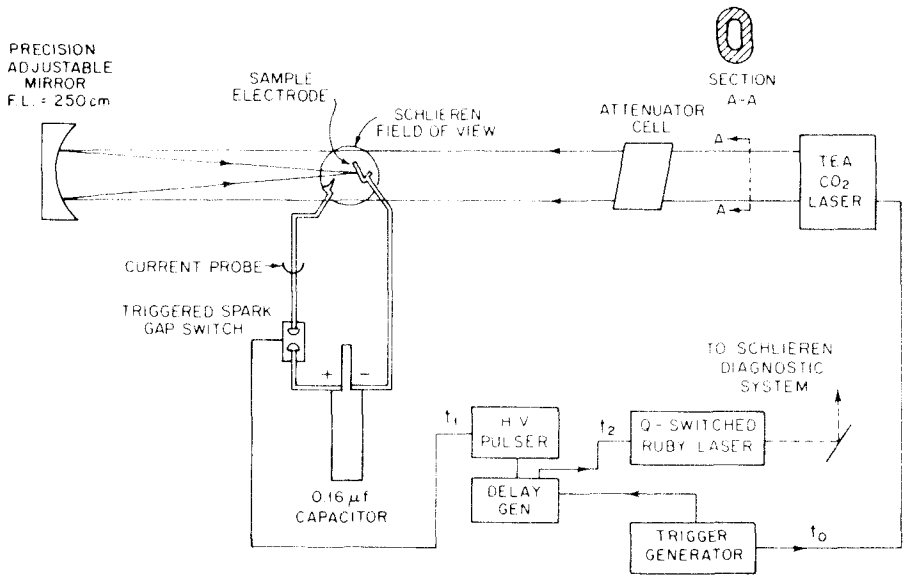

FIG. 1. Experimental configuration. The location of the focal spot on the sample is changed by adjusting the focusing mirror.

lem of self-breakdown of the interelectrode gap at the edges of the metal sample.

The discharge capacitors were charged to 30 kV and switched through a precision triggered spark gap (SG) switch. The low inductance discharge circuit was constructed using 10-cm-wide copper foil; thus, the circuit resistance during discharge (about 0.2 Ω) was primarily due to the resistance of the spark gap switch, the interelectrode gap, and the resistance at the surface of the electrodes. The left electrode was a pointed screw, while the right electrode consisted of the polished stainless-steel sample, which, in the hole boring experiments, was covered with aluminum foil. The size and shape of the sample electrode was chosen to fit within the center of the annular shaped laser beam. The smooth, flat, sample electrode was tilted at an angle of 65° relative to the laser beam axis to prevent feedback into the laser. For these laser and discharge parameters, the guided discharge had a peak current of about 12 kA, a ringing frequency of 0.4 MHz, and an RLC damped energy deposition time of about 25 μs. At the end of the discharge, the capacitors retained a charging voltage of 18 kV, which was inadequate to breakdown both the spark gap switch and the interelectrode gap. Thus, the initial capacitively stored energy was 72 J, the final stored energy was 26 J, depositing a total energy of 46 J into the entire discharge circuit. One expects less than one-half of this energy to be deposited in the spark gap switch, which has a low resistance, large area, UV preionized discharge, leaving more than 23 J available to be deposited mainly in the interelectrode gap and at the electrodes.

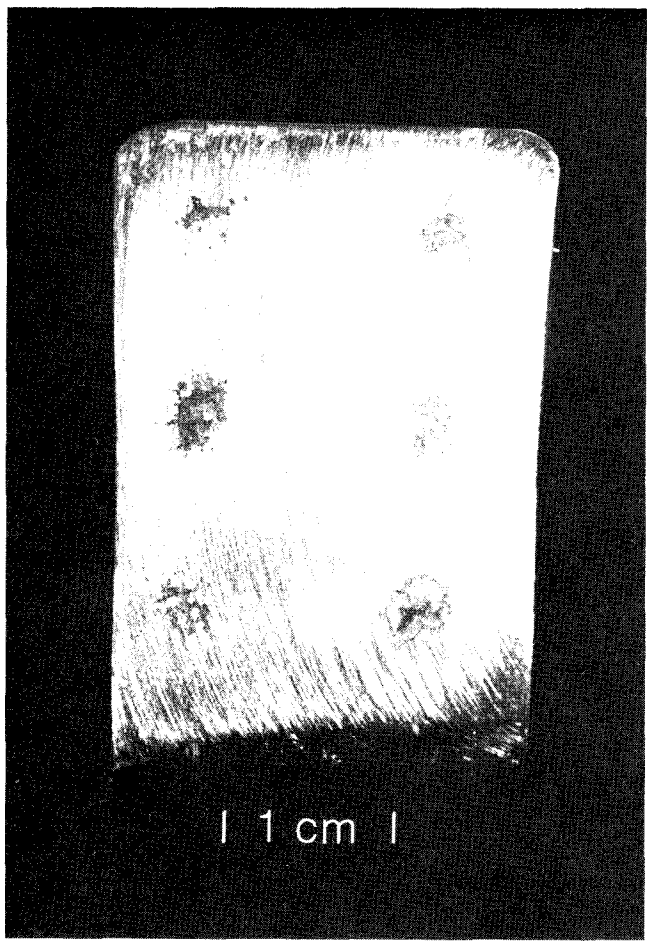

FIG. 2. Melted regions on the stainless-steel sample for seven separate laser guided discharges. Only the laser focal spot location on the sample was changed between shots. The left-center melted region was the result of two consecutive shots with the same focal spot location; each of the other melted regions are from a single shot. The delay between the CO_2 laser pulse and the discharge was 5 μs in all cases for this figure.

Discharge diagnostics included voltage, current, ruby laser Schlieren photography, and spectroscopy. The 20-ns pulsed ruby laser Schlieren photography system resembles one developed at the Naval Research Lab[10] and uses a small aperture instead of a knife edge. This results in a Schlieren photograph which measures the gradient of the density with two-dimensional resolution. The ruby laser was pulsed 1 μs after triggering the SG switch, so, including the sparkover time this was close to the peak of the current pulse and the instant of maximum ohmic power input. Spectroscopic measurements were made to determine the heating and ablation of the metal sample,

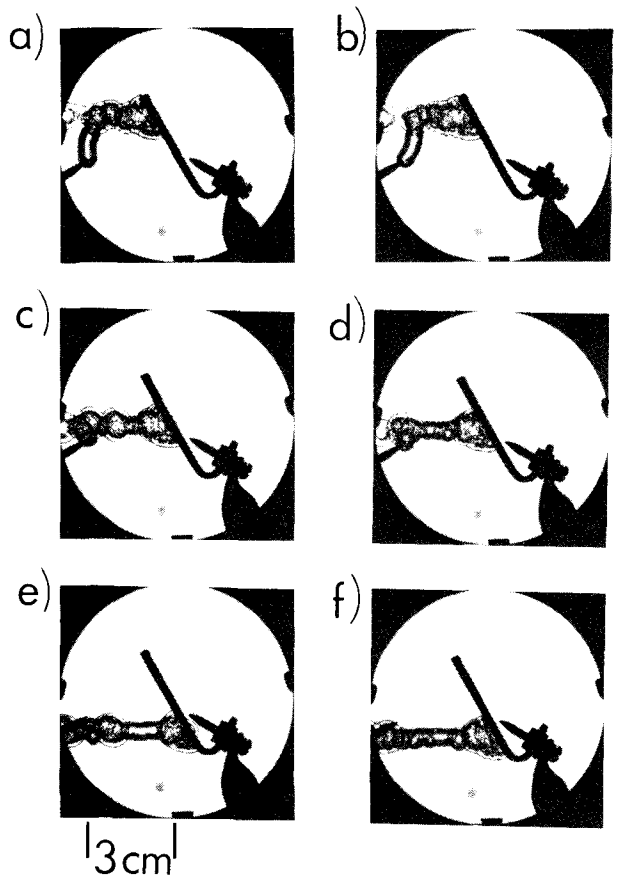

FIG. 3. Ruby laser Schlieren photographs of the same discharges shown in Fig. 2. The location of each of the Schlieren photographs in the figure corresponds to the location of the focal spot in Fig. 2, e.g., Fig. 3(a) corresponds to the top left melted region in Fig. 2.

however, line radiation from atmospheric nitrogen and oxygen overwhelmed any iron line radiation.

II. EXPERIMENTAL RESULTS AND DISCUSSION

A number of experiments were performed to investigate the process of localized metallic melting and to demonstrate the applicability of this process to machining of materials. Effects which have been studied included: (1) scannability of laser guided discharge melting on a metal sample by changing only the laser focal spot location, (2) dependence of the melted spot size and shape upon the delay between the CO_2 laser pulse and the high-voltage pulse, (3) the relationship between the region melted by the laser guided discharge and the laser focal pattern, and (4) the discharge energy deposition required to bore holes in thin aluminum foils.

Metallic melting (Fig. 2) and Schlieren photography data (Fig. 3) conclusively demonstrate that the LGD melting location could be controlled by changing only the location of the laser focal spot. The sample was held fixed while the laser focal spot was scanned in an array by adjusting the focusing mirror from shot to shot. The Schlieren photographs of the discharge show that the discharge path is well guided by the laser preionized channel. In Figs. 3(a) and 3(b) one can observe the discharge arcing nearly vertically (smooth curve) through the undisturbed air to meet the conducting path ionized by the laser induced breakdown (jagged curve). This clearly demonstrates that laser guided discharge machining could readily be automated by modulating the mirror focal spot according to a preset program. The left-center spot in Fig. 2 represents LGD melting for which two consecutive discharges were guided to the same spot, testing the reproducibility of the technique.

The data of Figs. 2 and 3 were obtained for identical laser energy, discharge voltage, and CO_2 laser-discharge delay (5 μs), however, a distinct difference in the melting pattern is apparent between the different spot positions. This effect can be interpreted in terms of two possible causes:

(1) Different discharge path lengths (Fig. 3) are required to reach the sample electrode, depending upon the

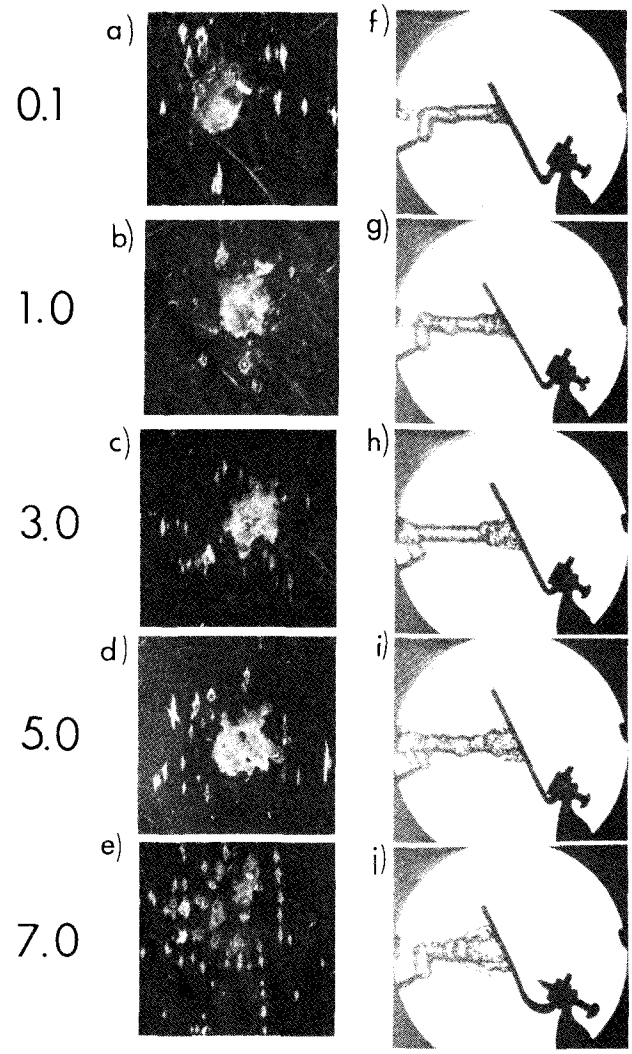

FIG. 4. Data which illustrate the effect of changing the relative timing of the CO_2 laser pulse and initiation of the discharge. Figures 4(a)–4(e) are photographs of the melted regions on a stainless-steel sample. Figures 4(f)–4(j) are Schlieren photographs corresponding to each of the discharges. The relative delay between the CO_2 laser pulse and the discharge is given in microseconds to the left of each row. The laser focal spot location was the same in each case; separate electrodes were used for each shot.

FIG. 5. Melted pattern on a stainless-steel sample from a single laser guided discharge in which the laser was defocused on the sample. Delay between the CO_2 laser pulse and the discharge was 5 μs.

spot position relative to the left-hand electrode. The longer discharge paths will have higher resistance and increased ohmic energy dissipation in the air, with lower energy available for metallic melting in the sample.

(2) Differences in the energy deposition profiles are also expected because the symmetry of the laser focal spot is degraded when the beam is scanned an appreciable distance off axis.

The dependence of the LGD melted spot diameter upon the relative timing of the CO_2 laser pulse and the application of the discharge voltage is shown in the photographs of Figs. 4(a)–4(e). Schlieren photographs of the same discharges, given in Figs. 4(f)–4(j), clearly show that as the delay between the CO_2 laser pulse and the discharge voltage is increased, the laser breakdown beads expand, increasing the diameter of the laser-ionized path. It is thus expected that the smallest LGD melted regions will be generated when the delay between the CO_2 laser and the discharge voltage is minimized. This effect is apparent in the data of Figs. 4(a)–4(e) in which the smallest discharge diameter and the best localized melting correspond to the shorter delay times, while the longer delay times exhibit larger diameter discharges and more diffuse melted regions. Possible means of further enhancing this effect by longer laser pulses which persist during the discharge are discussed later in this article.

A number of pits are seen in Fig. 4 to occur randomly outside the LGD melting spot. This effect is believed to be caused by small arcs outside the main discharge. These outer arcs could be randomly guided by filamentation or self-focusing caused breakup of the intense laser beam in the dense air-breakdown plasma. Further experiments are necessary to definitively identify the cause of this off-axis pitting.

The effect of defocusing the laser beam upon LGD melting of the electrode is apparent in Fig. 5. In this case, the defocused beam profile resembles a small annulus, accounting for the annular pattern of deep craters, which occur in place of a single main central melted region for the well-focused case.

Hole boring by laser guided discharges is demonstrated in Fig. 6. This was accomplished by covering the stainless-steel electrode with thin aluminum foil. For the 64-μm-thick foil, the hole diameter is about 1 mm [Fig. 6(a)], while for identical laser conditions a 4–5-mm-diam hole is bored in 38-μm-thick aluminum foil [Fig. 6(b)]. Again, the laser alone produced no discernable foil damage, ex-

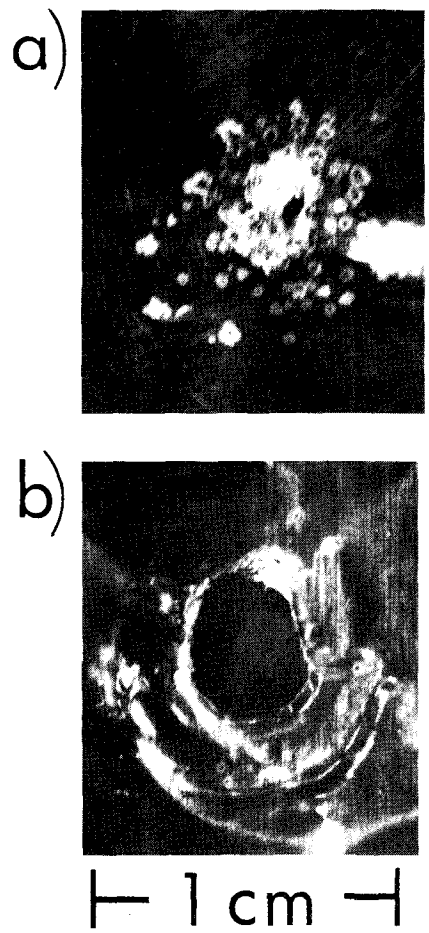

FIG. 6. Hole boring of aluminum foils by laser guided discharges: (a) 64-μm foil thickness, and (b) 38-μm foil thickness. Each hole was melted by a single laser guided discharge.

cept a small dent in the foil from the air-breakdown shock wave.

These data permit an estimate of the minimum discharge energy deposited in the foil, since the energy required to melt the displaced mass of aluminum can be calculated. This calculation yields a minimum LGD energy deposition in the 38-μm aluminum foil of about 1 J; for the 38-μm foil this energy estimate based on melting may be too high, because the aluminum appears to be pushed outward by the shock wave from the discharge. A similar analysis of the energy required to melt the hole in the 64-μm aluminum foil samples [Fig. 6(b)] yields a minimum energy deposition of 0.2 J.

Another estimate of LGD energy deposition in the aluminum samples can be performed by integrating the ohmic energy deposition E_Ω to the melted region

$$E_\Omega = \int_0^{25\ \mu s} i^2 R_f\, dt, \tag{1}$$

where i is the measured discharge current and R_f is the resistance of the foils; both foils are thinner than the skin depth at 0.4 MHz.[11] The results are a deposited LGD ohmic energy on the 38-μm foil of 0.15 J and for the 64-μm foil, 0.25 J. These estimates are in good agreement with the melting energy (E_m) for the 64-μm foil.

The efficiency (η) of the LGD energy deposition in the metal samples may thus be defined as

$$\eta = E_d/(E_i - E_f), \tag{2}$$

where E_i is the initial stored energy in the capacitors and E_f is the final energy stored in the capacitor after the discharge interupts. For our experimental parameters

$$E_i = 72\ \text{J},$$

$$E_f = 26\ \text{J},$$

and E_d may be assumed to be between E_Ω and E_m. Note that here we have not included the laser energy which is deposited in the air. In an optimized experiment this laser energy could be a small fraction of the discharge deposited energy. Thus, for 0.2 to 0.25 J deposited energy, the LGD efficiency is in the range for the 64-μm foil;

$$\eta = 0.4\%\ \text{to}\ 0.5\%.$$

It may be possible in an optimized experiment to improve this efficiency to be competitive with laser machining in which the efficiency of the CO_2 laser itself is less than 30%. If the coupling efficiency (in simple laser machining), of radiation to the material is considered, then laser guided discharge machining appears to be a promising new technique.

There are a number of steps which we are taking to optimize the efficiency of metal removal by laser guided discharges. These include:

(1) Higher capacitance in the discharge circuit to maximize the discharge current, pulse length, and skin depth.

(2) Longer laser pulses which overlap or persist during the discharge to provide discharge guidance and focusing throughout the duration of the energy deposition.

(3) By operating at reduced pressures of air or other gases, self-focusing of laser radiation could be eliminated. Experiments at reduced pressures[12] have demonstrated that, with absorbing gases, 1-m discharges can be guided with only 40 kV. Laser guided discharge channels in inert gas at atmospheric pressure have been demonstrated elsewhere[10] and could be applied to LGD welding.

(4) Finally, it may be possible to adapt such a technique to a rapid repetition rate system or possibly even a cw configuration.

ACKNOWLEDGMENTS

We express our gratitude to P. Weber for photographing the samples. This research was supported by the U.S. Office of Naval Research under Project NR-012-756.

[1] J. R. Greig, D. W. Koopman, R. F. Fernsler, R. E. Pechacek, I. M. Vitkovitsky, and A. W. Ali, Phys. Rev. Lett. **41,** 174 (1978).
[2] D. W. Koopman, J. R. Greig, R. E. Pechacek, A. W. Ali, I. M. Vitkovitsky, and R. F. Fernsler, J. Phys. (Paris) Colloq. 7, Suppl. 7, **40,** 419 (1979).
[3] D. W. Koopman and K. A. Saum, J. Appl. Phys. **44,** 5328 (1973).
[4] K. A. Saum and D. W. Koopman, Phys. Fluids **15,** 2077 (1972).
[5] G. Yonas, Sci. Am. **239,** 50 (1978).
[6] P. A. Miller, R. I. Butler, M. Cowan, J. R. Freeman, J. W. Poukey, T. P. Wright, and G. Yonas, Phys. Rev. Lett. **39,** 92 (1977).
[7] J. R. Freeman, L. Baker, and D. L. Cook, Nucl. Fusion **22,** 383 (1982).
[8] N. Rykalin, A. Uglov, and A. Kokora, *Laser Machining and Welding* (Translation) (Pergamon, NY, 1971).
[9] N. U. Shankar and A. Krishnan, Indian J. Technol. **17,** 363 (1979).
[10] M. Raleigh, J. R. Greig, R. W. Pechacek, and E. Laikin, NRL Memorandum Report 4380, 1981.
[11] S. Ramo, J. R. Whinnery, and T. VanDuzer, *Fields and Waves in Communication Electronics* (Wiley, New York, 1965), p. 288.
[12] K. Imasaki, S. Miyamoto, T. Ozaki, H. Fujita, S. Nakai, and C. Yamanaka, J. Phys. Soc. Jpn. **50,** 3847 (1981).